

Strength analysis of polymeric films

A. H. Tsou, J. S. Hord, G. D. Smith and R. W. Schrader

*Manufacturing Research and Engineering Organization, Eastman Kodak Company,
Rochester, NY 14652-3701, USA*

(Received 18 March 1991; revised 20 August 1991; accepted 28 August 1991)

In a simple and direct manner, residual strengths of edge-notched gelatin and cellulose acetate (CA) films under tension have been related to a single stress intensity factor. The effective stress intensity factors, or the effective fracture toughnesses, of the 0.012 mm gelatin and 0.13 mm CA films are 2.97 and 3.30 MN m^{-3/2}, respectively. Plasticity and finite width effects of edge-notched films are accommodated based on the Feddersen analysis. Stable crack growth before the fracture instability was confirmed using a high-speed video camera. Since stable crack extension guarantees the generation of naturally sharp cracks, sharp notches by fatigue cracking are not necessary for the fracture toughness measurement of thin films. However, with all the specimen widths employed (15–100 mm) edge-notched poly(ethylene terephthalate) (PET) films of 0.10 mm thickness showed net section yielding during fracture testing. This indicates that the fracture behaviour of PET films with widths up to 100 mm have to be analysed on the basis of the elastic–plastic fracture mechanisms, and the fracture toughness of PET film is much greater than 25.3 MN m^{-3/2}.

(Keywords: stress intensity factor; residual strength analysis; PET; cellulose acetate; gelatin; polymeric film; fracture toughness)

INTRODUCTION

Fracture toughness of polymeric films is of critical importance in a variety of film transporting and finishing operations. The fracture strength of thin polymeric films have been studied traditionally by the trouser leg tear test^{1–8}, especially for rubber. However, due to the mixed-mode fracture nature of the tear test⁹, the fracture strength thus determined can only provide a qualitative comparison of toughness between notched materials. Since the failure of films during film transporting and finishing is generally caused by mode I tensile fracture, it is necessary to examine the residual strength of notched polymeric films under tensile loading.

The mode I fracture toughness of polymeric films can be measured using either a centre-cracked or an edge-notched film specimen under uniaxial tension. The fracture toughness thus determined is K_{1c} , where the subscript 1 stands for mode I, plane stress fracture toughness. The plane stress condition arises from the fact that the plastic zone sizes of gelatin and cellulose acetate (CA) films examined in this study are larger than their respective thicknesses (see Results and Discussion). When the plastic zone is larger than the film thickness, yielding can take place freely in the thickness direction and the state of stress at the crack tip is in plane stress.

Under the plane stress condition, slow crack growth was observed to precede the onset of crack instability on a centre-cracked tension panel with constant displacement¹⁰. According to the energy concept^{11,12}, there is a continuous balance between the released strain energy, G , provided by the external force, and the consumed energy (or the crack resistance), R , during the slow stable crack growth. Here, the crack resistance represents the work needed for formation of a new plastic zone at the tip of the advancing crack. Since the load has to be raised

to sustain the stable crack growth, R is not a constant under the plane stress condition. It increases as the crack proceeds, from the initial crack length a_0 to the critical crack length a_c . The final fracture condition for the onset of crack instability at $a = a_c$ is:

$$G = R \quad \text{and} \quad \frac{\partial G}{\partial a} = \frac{\partial R}{\partial a} \quad (1)$$

where a is the crack length.

Based on experimental observations¹³, a_c at the point of fracture instability is approximately proportional to a_0 :

$$a_c = \alpha a_0 \quad (2)$$

For the case of $\alpha = 1$, R is a constant and there is no slow crack growth. For a brittle material in plane strain, $\alpha = 1$. Since a_c is related to a_0 , either one of the following expressions can be used for the stress intensity factor¹³:

$$K_{1c} = \beta \sigma_c \sqrt{\pi a_c} \quad K_{1e} = \beta \sigma_c \sqrt{\pi a_0} \quad (3)$$

where β is a factor that depends upon sample geometry and size. For a side-notched specimen¹³, $\beta = 1.12$, σ_c is the critical stress at fracture instability, K_{1c} is the critical stress intensity factor, or the fracture toughness, and K_{1e} is the effective fracture toughness.

However, it is immaterial that the plane stress crack grows slowly to a_c before fracture. The load that causes the material to fail under the presence of a given crack, a_0 , is the one that matters. Therefore, the residual strength should be calculated on the basis of K_{1e} not K_{1c} for which the measurements of a_c are difficult. To a first approximation, it can be assumed that the fracture behaviour in plane stress is dictated by the stress intensity factor. This is to state that the similitude on the basis of K is maintained or the plastic zone is smaller than the

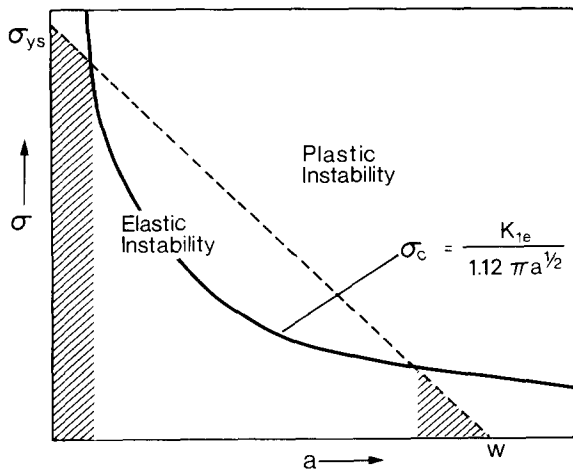


Figure 1 Residual strength characteristics in plane stress

crack size at all conditions. However, for films with narrow width or a film with very short or long crack in comparison with its width, general yielding can occur and the similitude condition is lost.

Fedderson¹⁰ has proposed a method of data analysis that extends the stress intensity factor concept to account for the full range of crack lengths and sample widths. Fedderson's analysis has been successfully applied to centre-cracked aluminium alloy panels^{10,13} over the whole range of flaw sizes and, in the process, the panel width effects were uncoupled from the crack behaviour. In this study, Fedderson's analysis of centre-cracked panels is applied to examine the fracture process of single-edge-notched (SEN) polymeric films. The construction of the complete stress-flaw size curve for SEN specimens, which differs only slightly from the original analysis by Fedderson for centre-cracked panels, is discussed in the following section. Based on the literature information available, we believe this to be the first attempt to apply Fedderson's analysis to polymeric films.

Residual strength analysis of SEN films

For films wide enough to produce the real *K*, the relationship between the residual strength and the crack length can be represented by the curve shown in Figure 1. Also shown is a straight line representing the net section yielding for which the condition can be written as

$$\sigma = \sigma_{ys}(1 - a/W) \tag{4}$$

where σ_{ys} is the yield stress and *W* is the film width. Under the conditions of net section yielding, the plastic zone spreads through the entire uncracked ligment, as shown in Figure 2, and the plastic deformation at the crack tip can occur freely. The shaded areas indicated in Figure 1 represent the regions of crack sizes at which stresses of the whole section would have to be above yield in order to cause fracture at the given *K*. Since stresses above yield cannot occur, fracture in these regions take place at stresses lower than those predicted by *K*. The deviations noted at small crack sizes, or at high stress levels, are known as plasticity effects. The deviations at relatively long crack lengths are known as finite width or boundary effects.

Many theoretical analyses have been developed and utilized to account for both of these effects, but they failed to consolidate the data into a meaningful form over the

full range of cracks. Fedderson¹⁰ proposed the use of the two linear tangents to the idealized *K* curve to establish a continuous curve for the residual strength. Using Fedderson's approach, one can draw a tangent to the SEN *K* curve from the point $a = W$, and the other tangent is drawn from the point $\sigma = \sigma_{ys}$. Since the first tangent has to go through (σ, σ_{ys}) , the tangency point at small crack sizes can be shown to be

$$\sigma = \frac{2}{3} \sigma_{ys} \tag{5}$$

For the second tangent to go through $(0, W)$, the tangency point at large crack sizes is

$$a = W/3 \tag{6}$$

Here, the stress intensity factor used for the SEN specimens is:

$$K = 1.12 \sigma_c \sqrt{\pi a_0} \tag{7}$$

where the factor 1.12 arises from the free edge stress correction¹⁴.

Using the tangency conditions, the screening requirements for valid plane stress fracture toughness testing using SEN specimens are:

$$\sigma_c < \frac{2}{3} \sigma_{ys} \quad \text{and} \quad a < W/3 \tag{8}$$

where the net section yielding is avoided. It should be emphasized that the two tangents used to present the data over the full range of crack sites have no physical basis¹³. However they are useful in an engineering analysis.

In the case of materials with very high toughness, as shown in Figure 3, net section yielding would occur at all crack sizes. By increasing the sample width, one may eventually interact the elastic instability (*K*) curve. The minimum width required for obtaining the valid fracture toughness can be determined from the SEN *K* curve, as shown in Figure 3:

$$W_{min} = \frac{27}{5.0176\pi} \left(\frac{K_{1c}}{\sigma_{ys}} \right)^2 \tag{9}$$

Buckling of the film may occur during plane stress fracture testing of materials with high fracture toughness. The buckling arises from the non-singular, compressive stress term in the equations for the crack-tip stress field in uniaxial tension¹³. Generally, a single column buckling

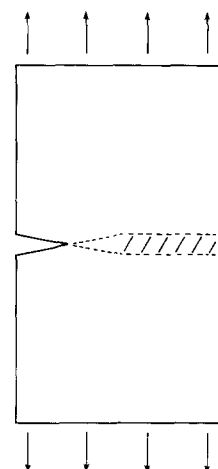


Figure 2 Fracture beyond general yield

formula is used to calculate the buckling stress¹⁵. Since the compressive stress along the crack edge is equal to the nominal uniform stress, buckling commences when :

$$\sigma = \frac{\pi^2 EB^2}{48 l^2} \quad (10)$$

This is the Euler formula for buckling a column of thickness B , modulus E and effective length l . The effective length l is related to a by⁶:

$$l = 0.5a \quad (11)$$

Equation (10) is used in this study to examine the buckling possibility during the fracture test of polymeric films. However, no antibuckling guides were applied during the test.

EXPERIMENTAL

Materials

A cast production-grade CA (degree of substitution = 2.85) film (Eastman Kodak Company) was used for this

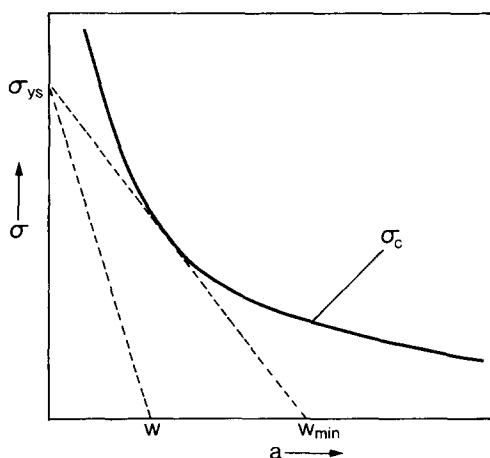


Figure 3 Residual strength of films with various widths

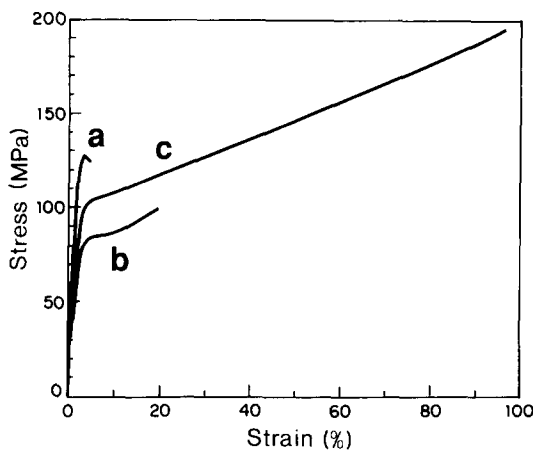


Figure 4 Stress-strain curves of (a) 0.012 mm thick gelatin film, (b) 0.13 mm thick CA film and (c) 0.10 mm thick PET film

Table 1 Mechanical properties of test films

Material	Thickness (mm)	E (GPa)	σ_{ys} (MPa)	σ_b (MPa)	ϵ_b (%)
CA	0.13 (1.8×10^{-3})	4.06 (0.058)	85.2 (0.90)	102.8 (7.10)	21.3 (4.9)
Gelatin	0.012 (7.6×10^{-4})	5.61 (0.261)	115.1	115.4 (6.69)	4.7 (2.0)
PET	0.10 (5.1×10^{-4})	4.83 (0.049)	105.3 (0.41)	198.6 (6.34)	99.0 (5.6)

Standard deviation in parentheses

study. The film is 0.13 mm thick and is plasticized with 12 wt% triphenyl phosphate. Standard 0.1 mm thick production-grade poly(ethylene terephthalate) (PET) film (ESTAR®, Eastman Kodak Company) was also used for evaluation. The PET film was biaxially stretched and heat set. Non-crosslinked gelatin, a lime-processed demineralized ossein extract produced by Rousselot Gelatin, was coated on a PET support, dried, conditioned at 21°C and 50% relative humidity, and then peeled off for testing. The coated gelatin film is 0.012 mm thick and was chill set at 4°C for 35 s, dried at 21°C for 120 s, and at 38°C for 295 s. A Sintech automated tensile tester (Sintech Corp., Stanton, USA) was used for the determination of the tensile properties of gelatin, CA and PET films. Samples were cut in the machine direction and were conditioned and tested at 21°C and 50% relative humidity at a strain rate of 50% min⁻¹. The characteristic stress-strain curves of these films are shown in Figure 4, and the corresponding mechanical properties are listed in Table 1.

Residual strength testing

An edge notch was manually placed in each sample using a sharp razor blade. The sample size was 15 mm × 138 mm, and the notch length varied from 0.38 to 12.7 mm. The notch lengths were measured using an optical microscope at 100× magnification. The general shape of the notch is shown in Figure 5. The notched samples were conditioned at 21°C and 50% relative humidity for a minimum of 24 h prior to testing.

Five samples of each notch length were tested with the Sintech tensile tester at 21°C and 50% relative humidity. It is necessary to reduce the size of the load cell as the notch length increases to ensure adequate sensitivity of the load signal. Pneumatic C-grips with a 25.4 × 38.1 mm² flat face and a line face were used with the 222 and 445 N load cells. A 25.4 × 50.8 mm² piece of blotter paper was placed between the sample and the line face to reduce slippage. Lighter weight grips with two 25.4 mm square flat faces were used with the 22.2 N load cell. The gauge length used for all samples was 102 mm and the strain rate was 50% min⁻¹. The critical stress value was taken at the peak load.

An Ektapro 1000 (1000 frames s⁻¹) camera was mounted in front of the Sintech tensile tester to examine stable crack growth. A white reflective surface was placed behind samples for lighting. To evaluate the deformation field during loading, crossed polars with a white light source were employed.

RESULTS AND DISCUSSION

Plane stress

If it is assumed that linear elastic fracture mechanics (LEFM) can be applied to the gelatin and CA films, the Irwin plane stress plastic zone size⁴, r_p , is:

$$r_p = \frac{\sigma^2 a}{\sigma_{ys}^2} \quad (12)$$

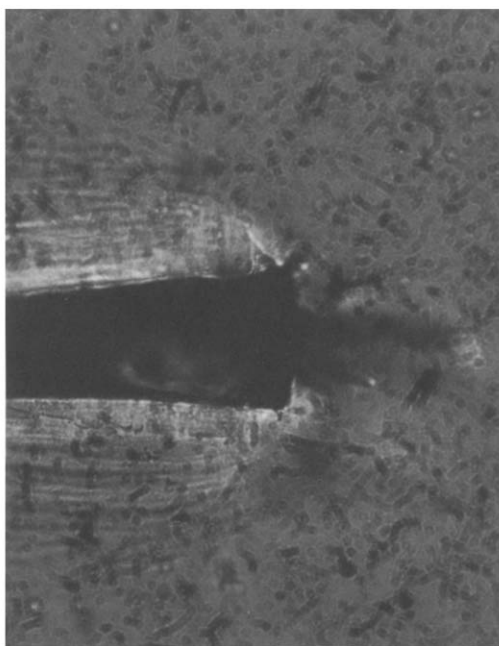


Figure 5 Photomicrograph of a notch on a 0.13 mm thick CA film

Using the critical stresses measured at given crack sizes, r_p for each individual polymer film examined is greater than the film thickness. For example, the plastic zone size for the gelatin with a 0.94 mm side crack is 0.203 mm and the plastic zone size for the CA film with a 0.838 mm side crack is 0.305 mm. This means that the stress for gelatin and CA films are plane stresses.

Residual strength analysis of gelatin and CA films

As shown in Figures 6 and 7, stable slow crack growth was observed to precede fracture instability for the CA film. The a_c is proportional to a_0 with the proportionality factor α being ~ 1.70 . Since stable crack growth provides a naturally sharp crack, unlike the plane strain specimen, the plane stress specimen need not be fatigue cracked. The calculated residual strength curves based on only one set of data at a given crack length for both gelatin and CA films are shown in Figures 8 and 9 together with the experimental data. The experimental points consist of data obtained in two separate experiments. It is obvious that the Feddersen analysis can account for the stress-flaw size relationship for the full range of crack lengths for the gelatin and CA films.

Net section yielding of the PET films

From the video of the 15 mm wide PET film under the cross-polarized light, it is indicated that a large deformation field is ahead of the crack tip and spreads towards the edge of the PET film (Figure 10). Therefore, the general yield is assumed for SEN PET film of 15 mm width. As shown in Figure 11, the critical stresses of all crack sizes follow the straight line of the general yield. Buckling of the PET film was also observed during the residual strength analysis. For the PET film with a 0.89 mm side crack, the buckling stress calculated from equation (10) is 52.4 MPa which is smaller than the critical stress of 96.5 MPa. By increasing the film width up to 100 mm, net section yielding is still indicated experimentally. This means that the minimum width required for the determination of PET fracture toughness

is > 100 mm. If 100 mm were used in equation (9) as the width, it is estimated that the fracture toughness of 0.10 mm thick PET film would have to be $> 25.3 \text{ MN m}^{-3/2}$.

CONCLUSIONS

The residual strengths of single-edge-cracked gelatin and CA films for the full range of crack sizes were established based on a single effective stress intensity factor. The effective stress intensity factors of the 0.012 mm gelatin and 0.13 mm CA films are 2.97 and $3.30 \text{ MN m}^{-3/2}$, respectively. Using this stress intensity factor, the stress-flaw size curve can be constructed for either gelatin or CA film with any film width or flaw geometry. For

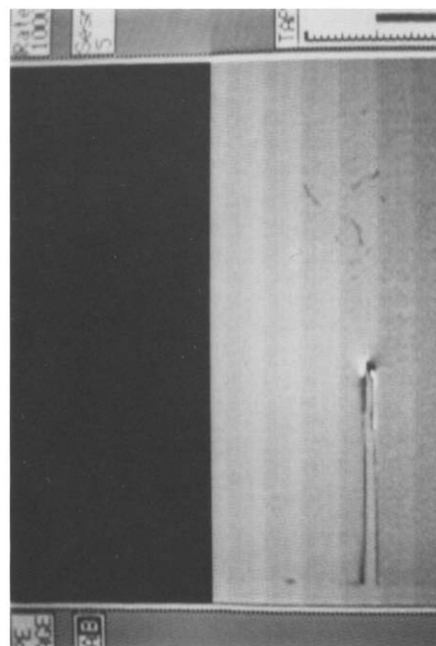


Figure 6 Photomicrograph of a 2.3 mm long edge cut of the CA film at the onset of the stable crack growth

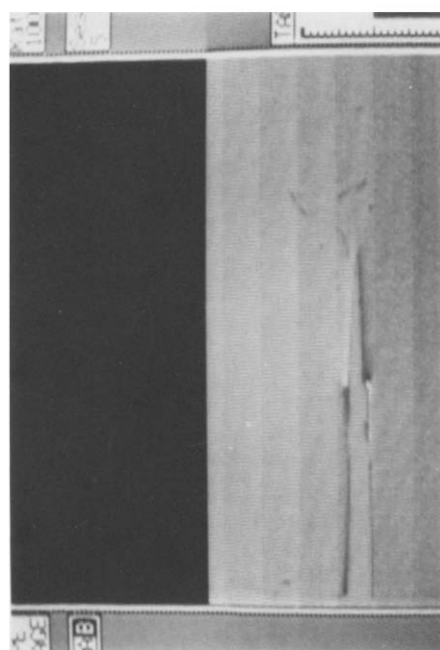


Figure 7 Photomicrograph of an edge cut of the CA film with 2.3 mm initial length at the onset of the crack instability

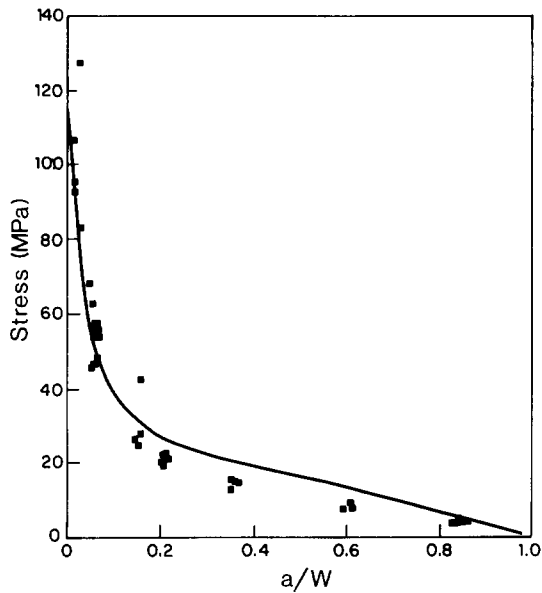


Figure 8 Residual strength of 0.012 mm gelatin film. Data (■) are compared with the prediction using Fedderson analysis (—)

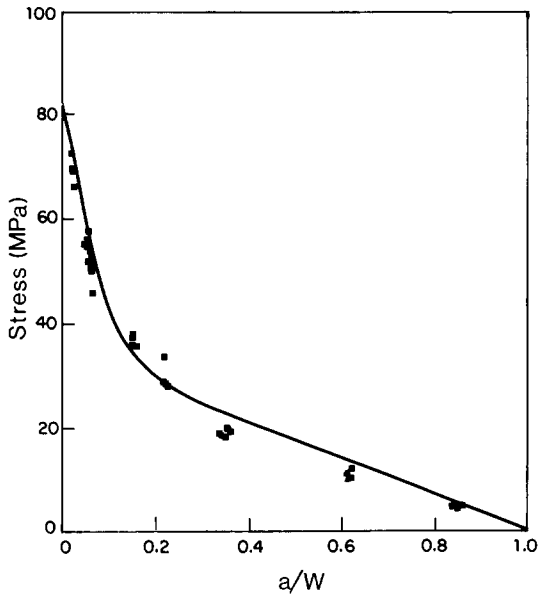


Figure 9 Residual strength of 0.13 mm CA film. Data (■) are compared with the prediction using Fedderson analysis (—)

PET, however, general yield was observed of the entire film during the fracture testing of films with widths that varied from 15 to 100 mm. This shows that the 0.10 mm thick PET film fails plastically and its LEFM fracture toughness, if obtainable, must be $>25.3 \text{ MN m}^{-3/2}$.

REFERENCES

- 1 Rivlin, R. S. and Thomas, A. G. *J. Polym. Sci.* 1953, **10**, 291
- 2 Thomas, A. G. *J. Polym. Sci.* 1955, **18**, 177
- 3 Greensmith, H. W. and Thomas, A. G. *J. Polym. Sci.* 1955, **18**, 189
- 4 Greensmith, H. W. *J. Polym. Sci.* 1956, **21**, 175
- 5 Thomas, A. G. *J. Polym. Sci.* 1958, **31**, 467
- 6 Anderton, G. E. and Treloar, L. R. G. *J. Mater. Sci.* 1971, **6**, 562
- 7 Sims, G. L. A. *J. Mater. Sci.* 1975, **10**, 647
- 8 Chiu, D. S., Gent, A. N. and White, J. R. *J. Mater. Sci.* 1984, **19**, 2622
- 9 Isherwood, D. D. and Williams, J. G. *Eng. Fracture Mech.* 1978, **10**, 887
- 10 Fedderson, C. E. ASTM STP 486, 1971, p. 50
- 11 Griffith, A. A. *Phil. Trans. R. Soc. London*, 1921, **A221**, 163
- 12 Irwin, G. R. *J. Appl. Mech.* 1957, **24**, 361
- 13 Broek, D. 'Elementary Engineering Fracture Mechanics', 4th Edn, Martinus Nijhoff Publishers, Dordrecht, 1986
- 14 Paris, P. C. and Sih, G. C. ASTM STP 391, 1965, p. 30
- 15 Dixon, J. R. and Strannigan, J. S. 'Fracture 1969', Chapman and Hall, London, 1969, p. 105

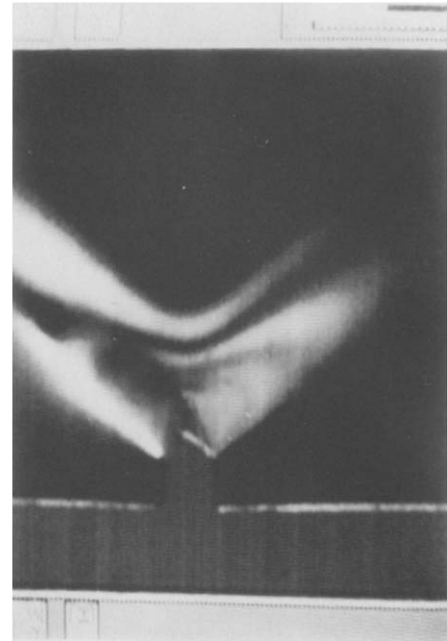


Figure 10 Birefringence pattern on the PET film with a uniform tensile load. The dark figures are 0° isoclinic lines

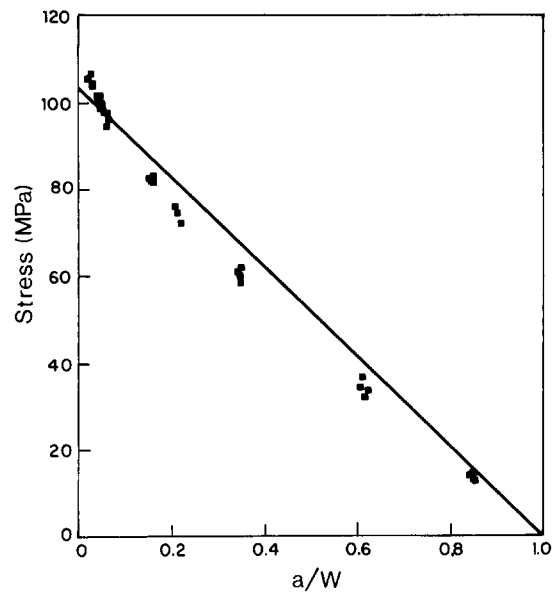


Figure 11 Residual strength of 0.10 mm thick PET film. Data (■) are compared with the general yield (—)